Original Article

Gut dysbiosis induced by a high-salt diet aggravates atherosclerosis by increasing the absorption of saturated fatty acids in ApoE-deficient mice

Takashi Yoshimura,[1] Takuro Okamura,[1] Hiroki Yuge,[1] Yukako Hosomi,[1] Tomonori Kimura,[1] Emi Ushigome,[1] Naoko Nakanishi,[1] Ryoichi Sasano,[2] Takehiro Ogata,[3] Masahide Hamaguchi,[1,*] and Michiaki Fukui[1]

[1]Department of Endocrinology and Metabolism and [3]Department of Pathology and Cell Regulation, Kyoto Prefectural University of Medicine, Graduate School of Medical Science, 465 Kajii-cho, Kamigyo-ku, Kyoto 602-8566, Japan
[2]AiSTI Science CO., Ltd., 18-3 Arimoto, Wakayama, Japan

(Received 18 September, 2024; Accepted 27 September, 2024; Released online in J-STAGE as advance publication 8 January, 2025)

Excessive salt intake has been associated with gut dysbiosis and increased cardiovascular risk. This study investigates the role of gut dysbiosis induced by a high-salt diet in the progression of atherosclerosis in ApoE-deficient mice. Sixteen-week-old male ApoE-deficient mice were fed either a high-fat, high-sucrose diet or high-fat, high-sucrose diet supplemented with 4% NaCl for eight weeks. The group on the HFHSD with high salt showed significant progression of atherosclerosis compared to the high-fat, high-sucrose diet group. Analysis of the gut microbiota revealed reduced abundance of beneficial bacteria such as *Allobaculum spp.*, *Lachnospiraceae*, and *Alphaproteobacteria* in the high-salt group. Additionally, this group exhibited increased expression of the Cd36 gene, a transporter of long-chain fatty acids, in the small intestine. Serum and aortic levels of saturated fatty acids, known contributors to atherosclerosis, were markedly elevated in the high-salt group. These findings suggest that a high-salt diet exacerbates atherosclerosis by altering gut microbiota and increasing the absorption of saturated fatty acids through upregulation of intestinal fatty acid transporters. This study provides new insights into how dietary salt can influence cardiovascular health through its effects on the gut microbiome and lipid metabolism.

***Key Words*:** **high-salt diet, gut dysbiosis, atherosclerosis, saturated fatty acids, ApoE-deficient mice**

Atherosclerosis is an inflammatory disease characterized by the accumulation of oxidized low-density lipoprotein (LDL) within the vascular intima, resulting in endothelial damage, upregulation of inflammatory cytokines, macrophage infiltration, intimal thickening, and subsequent plaque formation.[1,2] This condition is intricately linked to the onset of cardiovascular diseases (CVDs), which were the primary cause of mortality globally, accounting for approximately 32% of all deaths in 2019.[3]

Moreover, excessive dietary salt intake is a significant contributor to diabetes and hypertension, a well-established risk factor for atherosclerosis.[4,5] High salt consumption is also linked to alterations in the gut microbiota composition (dysbiosis), which compromises the intestinal epithelial barrier and promotes inflammatory cytokine production. A human study found that increased fecal salt levels correlated significantly with obesity and a reduction in beneficial gut bacteria, such as *Akkermansia muciniphila* and *Bifidobacterium*, including *Bifidobacterium longum* and *Bifidobacterium adolescentis*.[6] Additionally, research comparing the gut microbiota of hypertensive individuals with healthy controls demonstrated an elevated prevalence of the genus *Barnesiella* in those with hypertension.[7] Furthermore, animal studies have indicated that high salt intake disrupts intestinal microbiota composition in mice, aggravating colitis and reducing the relative abundance of lactobacilli and butyrate levels.[8] Chronic inflammation driven by inflammatory cytokines is a pivotal factor in the development of atherosclerosis.[1,9] Patients with inflammatory bowel disease (IBD) exhibit a two- to four-fold increase in the risk of myocardial infarction, stroke, and heart failure, as highlighted by cohort studies from Denmark and other European countries, which have shown a clear link between ischemic heart disease and IBD.[10–12] These findings underscore a strong connection between chronic intestinal inflammation and atherosclerosis; however, the specific mechanisms by which dysbiosis and intestinal inflammation induced by high salt intake contribute to atherosclerosis remain to be elucidated. LDL cholesterol is a recognized risk factor for atherosclerosis and CVDs, with diets high in saturated fatty acids elevating serum LDL cholesterol levels, thereby triggering inflammatory responses, abnormal lipid metabolism, and obesity.[13,14] Apolipoprotein E (ApoE) plays a crucial role in reducing plasma cholesterol levels and exerting anti-inflammatory effects, which inhibit atherosclerosis progression. ApoE-deficient mice are particularly susceptible to lipid dysregulation and atherosclerosis.[15] Furthermore, excessive saturated fatty acid intake is associated with atherosclerosis development, as these fatty acids are readily absorbed by cultured macrophages, potentially leading to increased arterial lipid deposition.[16]

Innate lymphoid cells (ILCs), which are immune cells lacking antigen receptors, are involved in innate immunity and have been implicated in various lifestyle-related, infectious, and allergic diseases. Notably, ILC2s have been reported to confer protection against atherosclerosis.[17] Our prior studies have demonstrated that dysbiosis resulting from a high-fat, high-sucrose diet induces intestinal inflammation, enhancing the gene expression of saturated fatty acid transporters in the small intestine epithelium, thereby increasing saturated fatty acid absorption, and worsening fatty liver disease.[18]

Based on these observations and our previous findings, we hypothesized that dysbiosis induced by a high-fat, high-sucrose,

*To whom correspondence should be addressed.
E-mail: mhama@koto.kpu-m.ac.jp

doi: 10.3164/jcbn.24-163

and high-salt diet might exacerbate atherosclerosis by modulating the expression of saturated fatty acid transporters in the intestinal tract. Consequently, this study aimed to elucidate the mechanisms through which excessive salt intake accelerates atherosclerosis and chronic inflammation by investigating changes in innate immunity and dysbiosis using a mouse model of atherosclerotic disease.

Materials and Methods

Mice. All animal experimental procedures were approved by the Committee for Animal Research, Kyoto Prefectural University of Medicine (M2021-56, 2021-107). Male B6.129P2-Apoetm1Unc/J (ApoE KO) mice were purchased from the Jackson Laboratory (Bar Harbor, ME) and bred in a specific pathogen-free room at this university. Gene disruption was performed by deleting parts of exon 3 and intron 3 of the mouse ApoE locus and inserting a neomycin resistance gene cassette from an *Escherichia coli* (*E. coli*) transposon (expressed under a polyomavirus enhancer sequence, an artificial translation starts site sequence, and a thymidine kinase gene promoter from herpes simplex virus) by homologous recombination.[19] The mice were 16-week-old at the beginning of the experimental procedures. Following many previous reports, we used 6- to 8-week-old ApoE KO mice, but since they did not show obvious atherosclerosis as previously reported, we increased the age of the mice from week to week and finally started experiments at 16 weeks. In addition, we have previously observed an increase in the phylum Proteobacteria and a decrease in the phylum Bacteroidetes in wild-type mice treated with HFHSD compared to mice treated with normal diet, as well as inflammation in the gut and an increase in saturated fatty acids in the serum to induce stronger metabolic abnormalities compared to normal diet.[20] Therefore, HFHSD was employed. They were fed for eight weeks either a high-fat high-sucrose diet (HFHSD; 20% protein, 40% carbohydrate, and 40% fat, coconut oil, 0.3% gm NaCl; D12327, Research Diets, Inc., New Brunswick, NJ) or HFHSD + excessive salt (4% gm NaCl). Paired feeding was performed by supplying an equal amount of feed. The mice were maintained in an environmentally controlled room (temperature, 23 ± 1.5°C; humidity, 40–60%; and a 12-h light/dark cycle, from 7 a.m. to 7 p.m). Cumulative oral intake was measured for 8 weeks. The manually weighed fresh food was placed in a trough in each cage once every three days at 9 a.m. and the amount of food was then measured after 24 h. The remnants of the chow were discarded. At 24 weeks of age, mice were fasted overnight and were then sacrificed by the administration of a combination of anesthetics: 4.0 mg/kg, midazolam, 0.3 mg/kg of medetomidine, and 5.0 mg/kg of butorphanol.[21] At the time of sacrifice, blood was collected by puncturing the left ventricle of the mouse. To remove circulating blood from the mice, the mice were slowly perfused with 10 ml of PBS from the left ventricle, then the epididymal adipose tissue, jejunum, and finally the aorta were dissected.

Blood pressure measurement. We assessed systolic blood pressures (SBP) and diastolic blood pressures (DBP) under anesthesia at 24 weeks of age using a mouse tail-cuff blood pressure monitor (BP-98AL V3.02; Softron Co. Ltd., Tokyo, Japan). To train and improve animal habituation, animals were placed in the holder for 15 min for 3 consecutive days prior to the actual test. The animal was placed in the holder and the tail was lifted and gently placed in the rear of the holder. Blood pressure was measured through the tail into the occlusion cuff. The mean blood pressure was calculated using the following formula (mean = diastolic pressure + 1/3 of pulse pressure).

Biochemistry. Blood samples were collected from fasted mice, and serum samples were collected after centrifugation at 14,000 rpm for 10 min at 4°C. The levels of triglycerides (TG) and total cholesterol (T-Chol)[22] were measured using the enzymatic method. Biochemical examinations were performed using a FUJIFILM Wako Pure Chemical Corporation (Osaka, Japan).

Arteriosclerotic area measurement. The atherosclerotic foci of the aortic annulus were used to measure the atherosclerotic area. Aortas were refluxed in phosphate-buffered hygienic saline, as previously reported, embedded in a frozen tissue embedding agent, fixed with dry ice, and frozen. Frozen sections were obtained using a cryostat until the aortic valve was visible and then sectioned serially at a thickness of 6 μm.[23] Ten sections per pull were examined.

Tissues were fixed in 60% isopropanol for 15 s and stained with oil red-O (Wako Pure Chemicals) for 30 min at room temperature. After staining, images were taken with BZ-X710 (Keyence Co., Osaka, Japan), and the arterial stiffness area was measured using ImageJ (ver. 1.54m, NIH, Bethesda, MD).

Isolation of mononuclear cells from aortas in mice. Using a dissecting microscope equipped with a cold light source (2.5× magnification), fatty tissue adjacent to the adventitia was carefully dissected and removed, leaving the outer aortic membrane intact. Lymph nodes near the aorta were carefully resected.

The entire aorta was harvested, and the plaque was detached from the intima. The aortic segment was placed in a 60 mm dish in ice-cold fluorescent activated cell sorting (FACS) buffer and stored until enzymatic digestion.

The aortas were transferred from a 60 mm dish to a 1.5 ml Eppendorf tube and 0.5 ml of an enzyme cocktail was added. The enzyme cocktail contained the following: 400 U/ml collagenase type I, 120 U/ml collagenase type XI, 60 U/ml hyaluronidase, 60 U/ml DNase1 (C0130, C765, H3506, and 11284932001, respectively; Sigma-Aldrich, St. Louis, MO); 20 mM HEPES (15630106; Gibco™, Thermo Fisher Scientific, Waltham, MA) and Dulbecco's phosphate-buffered saline containing calcium (DPBS, Thermo Fisher Scientific). The aortic tissue was cut into small pieces using scissors. The mixture was then transferred to a 50 ml Falcon tube and another 2 ml of the enzyme cocktail was added. The tubes containing the aortic tissue pieces were transferred to a water bath at 37°C for 50 min with slow shaking. After 50 min, the digestion solution was poured into a 100 μm cell strainer placed at the top of a new 50 ml Falcon tube. The remaining aortic tissue was crushed with a syringe plunger, and the cell strainer was rinsed with 5 ml FACS buffer. The filtrates were collected and centrifuged at 300 × *g* for 10 min at 4°C. The supernatant was carefully removed after centrifugation, and the cell pellet was suspended in 400 μl of FACS buffer.[24]

Tissue preparation and flow cytometry. Stained cells were analyzed using FACS Canto II, and the data were analyzed using FlowJo ver. 10 software (Ashland, OR). For gating of innate lymphoid cells, the following antibodies, purchased from eBioscience (Thermo Fisher Scientific), were used: Biotin-CD3e (100304; clone: 145-2C11; 1/200), Biotin-CD45R/B220 (103204; clone: RA3–6B2; 1/200), Biotin-Gr-1 (108404; clone: RB6-8C5; 1/200), Biotin-CD11c (117304; clone: N418; 1/200), Biotin-CD11b (101204; clone: M1/70; 1/200), Biotin-Ter119 (116204; clone: TER-119; 1/200Biotin-FceRIa (134304; clone: MAR-1; 1/200), FITC-Streptavidin (405202; 1/500), PE-Cy7-CD127 (135014; clone: A7R34; 1/100), Pacific Blue-CD45 (103116; clone: 30-F11; 1/100), PE-GATA-3 (clone: TWAJ, 1/50), APC-RORγ (clone: AFKJS-9, 1/50), and Fixable Viability Dye eFluor 780 (1/400).[25,26] Additionally, the following antibodies (also purchased from eBioscience) for gating of M1 and M2 macrophages were used: APC-CD45.2 (17045482; clone: 104, 1/50), PE-F4/80 (12480182; clone: BM8, 1/50), APC-Cy7-CD11b (47011282; clone: M1/70, 1/50), FITC-CD206 (MA516870; clone: MR5D3, 1/50), and PE-Cy7-CD11c (25011482; clone: N418, 1/50)[27] (Supplemental Fig. 1*).

Quantification of free fatty acids in the feces, aorta, sera, and white adipose tissue. Fatty acid composition in the feces, aorta, sera, and white adipose tissue (WAT) of ApoE KO mice

*See online. https://doi.org/10.3164/jcbn.24-163

was measured using gas chromatography-mass spectrometry (GC-MS) with an Agilent 7890B/7000D instrument (Agilent Technologies, Santa Clara, CA). Fifteen milligrams of aorta and feces and 25 μl of sera were methylated using a fatty acid methylation kit (Nacalai Tesque Inc., Kyoto, Japan). If the sample weight was less than 15 mg, the concentration was calculated by dividing by the weight. The final product was loaded onto a Varian capillary column (DB-FATWAX UI, Agilent Technologies). The CP-Sil 88 for the FAME capillary column was used for fatty acid separation (100 m × an inner diameter of 0.25 mm × membrane thickness of 0.20 μm; Agilent Technologies). The column temperature was maintained at 100°C for 4 min and then gradually increased by 3°C/min to 240°C, and held for 7 min. The sample was injected in the split mode with a split ratio of 5:1. Each fatty acid methyl ester was detected in the selected ion monitoring mode. All results were normalized to the peak height of the C17:0 internal standard.[28]

Quantitative real-time polymerase chain reaction (q-RT-PCR) of the aorta, jejunum, and white adipose tissue. Gene expression was analyzed using q-RT-PCR. Each aorta, jejunum, and WAT sample was homogenized in ice-cold QIAzol Lysis reagent (Qiagen, Hilden, Germany), and total RNA was isolated using the RNeasy MinElute Cleanup Kit (Qiagen), according to the manufacturer's instructions. Total RNA (0.5 μg) was reverse-transcribed using a High-Capacity cDNA Reverse Transcription Kit (Applied Biosystems, Waltham, MA) for first-strand cDNA synthesis, using an oligonucleotide dT primer and random hexamer primers according to the manufacturer's recommendations. The reverse transcription reaction was performed for 120 min at 37°C, and the enzyme was then inactivated by incubation at 85°C for 5 min. RT-PCR was performed using TaqMan Fast Advanced Master Mix (Applied Biosystems), according to the manufacturer's instructions. The following PCR conditions were used: one cycle of 2 min at 50°C and 20 s at 95°C, followed by 40 cycles of 1 s at 95°C and 20 s at 60°C.

Total RNA extracted from the aorta and jejunum was diluted to 5 ng/μl for all samples in DNase-RNase-free water after concentration measurement using Thermo Scientific™ NanoDrop Lite (Thermo Fisher Scientific). The relative expression levels of each target gene in the aorta [C-C motif chemokine ligand 2 (*Ccl2*), interleukin 1 beta (*Il1b*), interferon gamma (*Ifng*), tumor necrosis factor alpha (*Tnfa*), and interleukin 33 (*Il33*)], the jejunum [Cluster of differentiation (*Cd36*) and interleukin 22 (*Il22*)], and the WAT (*Ccl2*, *Il1b*, *Ifng*, and *Tnfa*) were normalized to the Glyceraldehyde 3-phosphate dehydrogenase (*Gapdh*) threshold cycle (CT) value and quantified using the comparative threshold cycle $2^{-\Delta\Delta CT}$ method as previously described.[29] We focused on the increase or decrease in fatty acid absorption. Since fatty acid absorption occurs mainly in the small intestine, we evaluated *Cd36* and *Il22* gene expressions in the jejunum instead of the colon in this study. Signals from HFHS-fed ApoE KO mice were assigned a relative value of 1.0. Six mice from each group were examined, and RT-PCR was performed in triplicates for each sample.

16S rRNA sequencing. Three 24-week-olds of middle weight in the group were selected, and microbial DNA was extracted from frozen fecal samples using the QIAamp DNA Feces Mini Kit (Qiagen), following the manufacturer's instructions. The V3–V4 region of the 16S rRNA gene was amplified from the DNA using a bacterial universal primer set (341F and 806R). PCR was performed with 20 ng of genomic DNA as a template in a 30 μl reaction mixture using EF-Taq (SolGent, Daejeon, South Korea) for the following cycles: activation of Taq polymerase at 95°C for 2 min, followed by 35 cycles at 95°C, 55°C, and 72°C for 1 min each, finishing with 10 min at 72°C. Amplification products were purified using a multiscreen filter plate (MilliporeSigma, Burlington, MA). 16S rRNA sequencing was performed using a MiSeq sequencer (Illumina, San Diego, CA) according to the manufacturer's instructions (Macrogen, Seoul, Korea). QIIME ver. 1.9.1 was used to filter sequences for quality.[30] Scores less than 75% and mismatches in the barcode or primers were eliminated from the files. The number of operational taxonomic units (OTUs) was determined using the UCLUST algorithm at 97% similarity.[31] Taxonomic assignment of 16S rRNA was performed with the Greengenes core-set-aligned with UCLUST and UNITE sequence sets for ITS using BLAST (UNITE, 2017). Based on a two-group comparison of the Bacteroidetes/Firmicutes ratio, the sample size was calculated to be 3 (35.9% difference in means between the two groups, 19.1% SD, alpha error 0.05, power 0.8).

The relative abundance of the phenotypic categories of the taxonomic groups was predicted using METAGENAssist, which is a statistical tool for comparative metagenomics.[32] Data filtering was based on interquartile range, row normalization by sum, and column normalization based on autoscaling. In addition, the Firmicutes/Bacteroidetes (F/B) ratio was calculated. Alpha diversity was defined as the diversity within an individual sample using the Shannon index,[33] Chao1,[34] and Gini-Simpson index.[35]

Moreover, differences in microbial communities between the two groups were investigated using the phylogeny-based weighted UniFrac distance metric and principal coordinate analysis (PCoA) plots, and non-hierarchical *K*-means cluster analysis was performed with the number of clusters to be generated pre-specified as two using the Tinn-R Gui ver. 1.19.4.7, R ver. 1.36.[36]

The relative abundance of phyla in the groups was evaluated by unpaired *t* test using the JMP ver. 13.2 software (SAS Institute Inc., Cary, NC). Furthermore, the relative abundance of bacterial genera between groups was evaluated using linear discriminant analysis (LDA) coupled with effect size measurements (LEfSe) (https://huttenhower.sph.harvard.edu/lefse/).[37] Using a normalized relative abundance matrix, LEfSe showed taxa with significantly different abundances, and the effect size of the feature was estimated using LDA. A p value threshold of 0.05 (Wilcoxon rank-sum test) and an effect size threshold of 2 were used for all biomarkers discussed in this study.

Statistical analysis. Data were analyzed using JMP ver. 13.0 software (SAS, Cary, NC). Differences between the two groups were compared using Welch's *t* test. Statistical significance was set at $p<0.05$, and asterisks were indicated in the figures as follows to express statistical significance; $*p<0.05$, $**p<0.01$, $***p<0.001$, and $****p<0.0001$. Statistical significance of body weight and oral intake were analyzed using two-way repeated measures ANOVA followed by Bonferroni's tests. Figures were generated using GraphPad Prism software (ver. 9.0; San Diego, CA).

Results

Effects of HFHSD with high-salt loading on body weight, serum lipids. ApoE KO mice were either fed with HFHSD + 4% NaCl or with HFHSD only, and their body weights, blood pressure, and serum lipid levels were compared. At 22 weeks of age, the HFHSD + 4% NaCl or group had significantly lower body weights than the HFHSD group (Fig. 1A). As shown in Fig. 1B, both groups were pair-fed with similar food intake.

The systolic, diastolic, mean blood pressure and pulse pressure were not different between the HFHSD and HFHSD + 4% NaCl groups (Fig. 1C–F). Serum lipid levels, such as TG and T-chol were investigated. The HFHSD + 4% NaCl group had higher serum TG and T-chol levels than the HFHSD group (Fig. 1G and H).

Effects of HFHSD with high-salt loading on atherosclerotic foci of the aortic annulus. Next, the area of arterial atherosclerosis in the aortic annulus was measured (Fig. 1I). The atherosclerosis area in the HFHSD + 4% NaCl group was larger

doi: 10.3164/jcbn.24-163

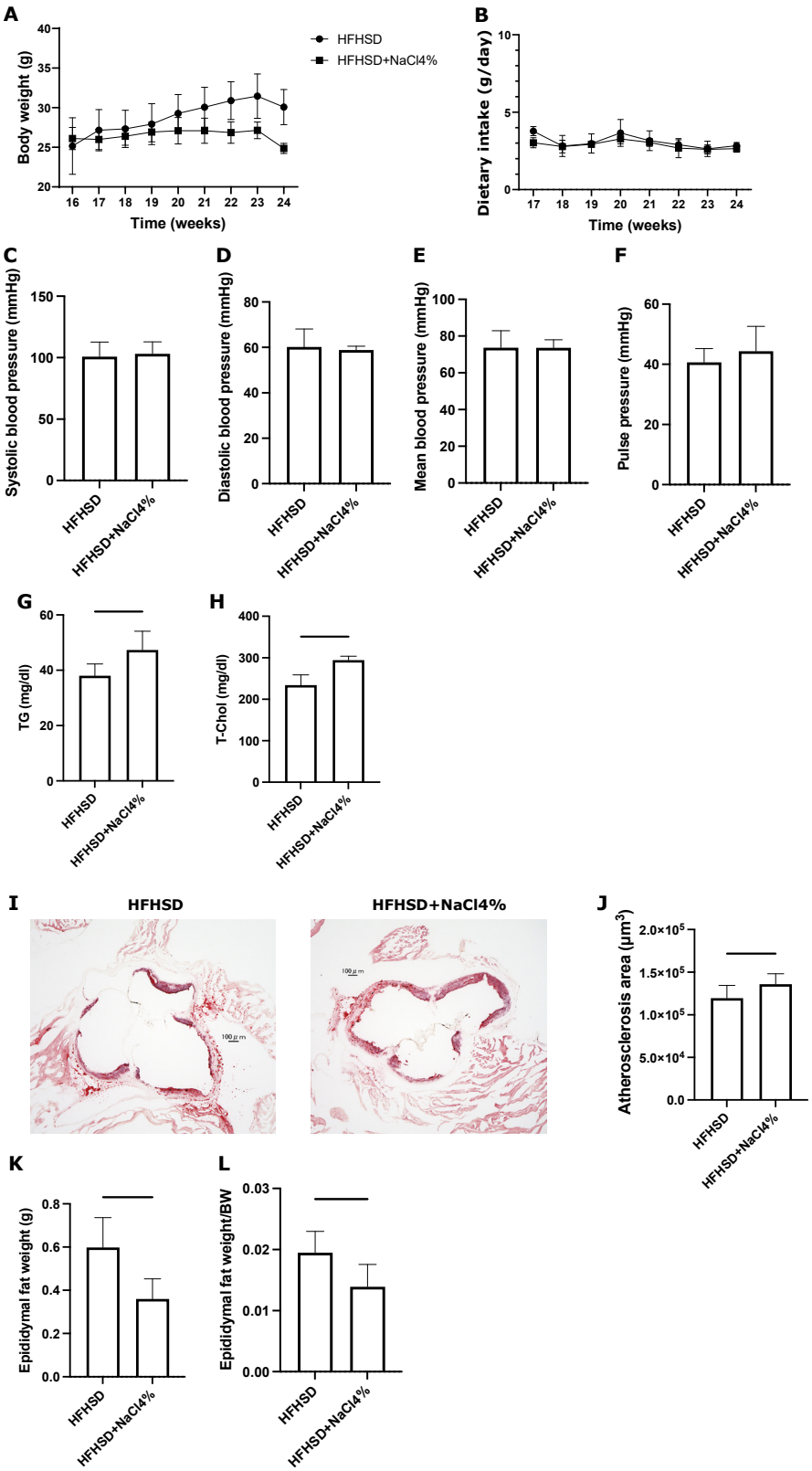

Fig. 1. Changes in body weight, blood pressure, blood biochemistry, and visceral fat weight in a mouse model of atherosclerosis. (A) Body weight changes in 16-week-old and 24-week-old ApoE KO mice fed with HFHSD and HFHSD + 4% NaCl ($n = 6$). Two-way repeated measures ANOVA followed by Bonferroni's tests (*$p<0.001$). (B) Dietary intake ($n = 6$). (C) Systolic blood pressure ($n = 6$). (D) Diastolic blood pressure ($n = 6$). (E) Mean blood pressure ($n = 6$). (F) Pulse pressure ($n = 6$). Serum levels of (G) TG and (H) T-Chol ($n = 6$). (I) Representative histological images of aortic valves stained with oil red-O. (J) Atherosclerosis area ($n = 6$). (K, L) Absolute and relative epididymal fat weight ($n = 6$). Data are presented as mean ± SD values and analyzed using Welch's t tests; *$p<0.05$, **$p<0.01$. HDL-Chol, high-density lipoprotein cholesterol; HFHSD, high-fat high-sucrose diet; HFHSD + 4% NaCl, HFHSD and 4% gm NaCl; LDL-Chol, low-density lipoprotein cholesterol; NEFA, non-esterified fatty acid; TG, triglycerides; T-Chol, total cholesterol.

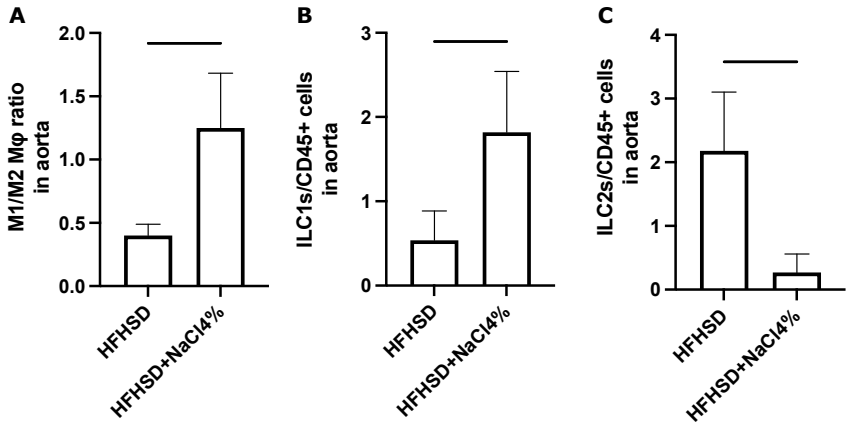

Fig. 2. Innate immune cells in the aorta. (A) M1/M2 macrophages ratio, (B) ILC1s/CD45 positive cells, and (C) ILC2s/CD45 positive cells in the aorta (n = 6). Data are presented as mean ± SD values and analyzed using Welch's t tests, *p<0.05. HFHSD, high-fat high-sucrose diet; HFHSD + 4% NaCl, HFHSD and 4% gm NaCl; ILC, innate lymphoid cells; Mφ, macrophages.

Table 1. Fatty acids in feces, aorta, and sera

	Feces (μmol/mg)			Aorta (μmol/mg)			Sera (μM)		
	HFHSD	HFHSD + 4% NaCl	p value	HFHSD	HFHSD + 4% NaCl	p value	HFHSD	HFHSD + 4% NaCl	p value
Saturated fatty acids									
Lauric acid	1.41 (0.10)	0.32 (0.08)	<0.001	7.10 (0.24)	9.63 (0.67)	0.007	24.18 (8.17)	52.20 (4.69)	0.014
Myristic acid	0.99 (0.04)	0.35 (0.07)	<0.001	6.03 (0.39)	8.37 (0.31)	0.003	16.50 (6.62)	34.94 (7.93)	0.065
Palmitic acid	30.92 (0.45)	14.39 (2.79)	0.028	12.09 (0.14)	16.27 (0.26)	<0.001	134.17 (14.00)	280.07 (44.57)	0.026
Stearic acid	0.93 (0.01)	0.73 (0.06)	0.033	4.00 (0.89)	6.77 (0.86)	0.034	38.23 (7.12)	93.08 (2.30)	0.018
Monounsaturated fatty acids									
Palmitoleic acid	0.61 (0.16)	0.08 (0.03)	0.011	4.59 (0.38)	5.34 (0.26)	0.083	8.30 (2.77)	36.13 (15.53)	0.067
Oleic acid	2.70 (0.19)	0.74 (0.29)	0.001	17.64 (1.25)	29.26 (0.92)	<0.001	114.96 (30.25)	234.43 (59.79)	0.065
Polyunsaturated fatty acids									
Linoleic acid	1.90 (0.29)	0.48 (0.17)	0.004	13.42 (3.31)	21.14 (1.02)	0.035	231.62 (62.26)	93.46 (10.17)	0.036
Gamma-linolenic acid	0.06 (0.01)	0.02 (0.01)	0.022	0.04 (0.01)	0.32 (0.37)	0.332	14.69 (2.38)	6.34 (0.63)	0.009
Alpha-linolenic acid	1.58 (0.63)	0.17 (0.03)	0.034	10.60 (5.23)	5.01 (3.18)	0.266	11.31 (1.61)	4.43 (0.340	<0.001
Dihomo-γ-linolenic acid	0.52 (0.11)	0.18 (0.11)	0.033	3.94 (1.07)	1.75 (0.32)	0.049	0.09 (0.03)	0.03 (0.02)	0.11
Arachidonic acid	0.13 (0.05)	0.04 (0.02)	0.12	0.93 (0.13)	2.00 (0.54)	0.054	75.98 (23.26)	16.63 (5.71)	0.028
Eicosapentaenoic acid	0.31 (0.09)	0.14 (0.01)	0.137	1.43 (0.10)	0.04 (0.01)	<0.001	104.46 (21.57)	53.31 (3.92)	0.03
Docosahexaenoic acid	0.74 (0.03)	0.08 (0.04)	<0.001	5.91 (0.75)	4.15 (0.63)	0.065	0.46 (0.06)	0.13 (0.05)	0.011

Data are expressed as mean (SD). Student's paired t test were conducted between two groups.

than that in the HFHSD group (Fig. 1J).

Effects of HFHSD with high-salt loading on the weight of visceral fat mass. To assess visceral fat mass, epididymal fat was adopted in this study and weighed (Fig. 1K and L). Absolute and relative weight of epididymal fat weight of the HFHSD + 4% NaCl group was lower than those of the HFHSD group.

Dynamics of inflammatory and anti-inflammatory cells in the aorta. Flow cytometric analysis was performed to determine the number of cells involved in innate immunity in the aorta in the two groups. The M1/M2 macrophage ratio in the aorta of the HFHSD + 4% NaCl group was higher than that of the HFHSD group (Fig. 2A). The percentage of ILC1 + $CD45^+$ cells of the aorta in the HFHSD + 4% NaCl group was higher than that in the HFHSD group (Fig. 2B), whereas that of ILC2 in $CD45^+$ cells was lower in the HFHSD + 4% NaCl group (Fig. 2C).

Saturated fatty acids in feces, sera, and aorta. The concentrations of saturated fatty acids, such as lauric, myristic, palmitic, and stearic acids, in feces, sera, and aortas were investigated by GC/MS. The concentration of saturated fatty acids in the feces of the HFHSD + 4% NaCl group was lower than that of the HFHSD group. On the other hand, the concentrations of saturated fatty acids in the sera and aorta of the HFHSD + 4% NaCl group were higher than those in the HFHSD group. A similar trend was observed in WAT (Supplemental Table 1*). In addition, the concentrations of monounsaturated fatty acids (MUFAs) and polyunsaturated fatty acids (PUFAs) in the feces and sera of the HFHSD + 4% NaCl group lower than those of the HFHSD group, whereas in aorta, the trends differed by fatty acid: linoleic acid, gamma-linolenic acid, and arachidonic acid were higher in the HFHSD + 4% NaCl group, while alpha-linolenic acid (ALA), dihomo-γ-linolenic acid, eicosapentaenoic acid (EPA), and docosahexaenoic acid (DHA) were higher in the HFHSD group (Table 1).

*See online. https://doi.org/10.3164/jcbn.24-163

doi: 10.3164/jcbn.24-163

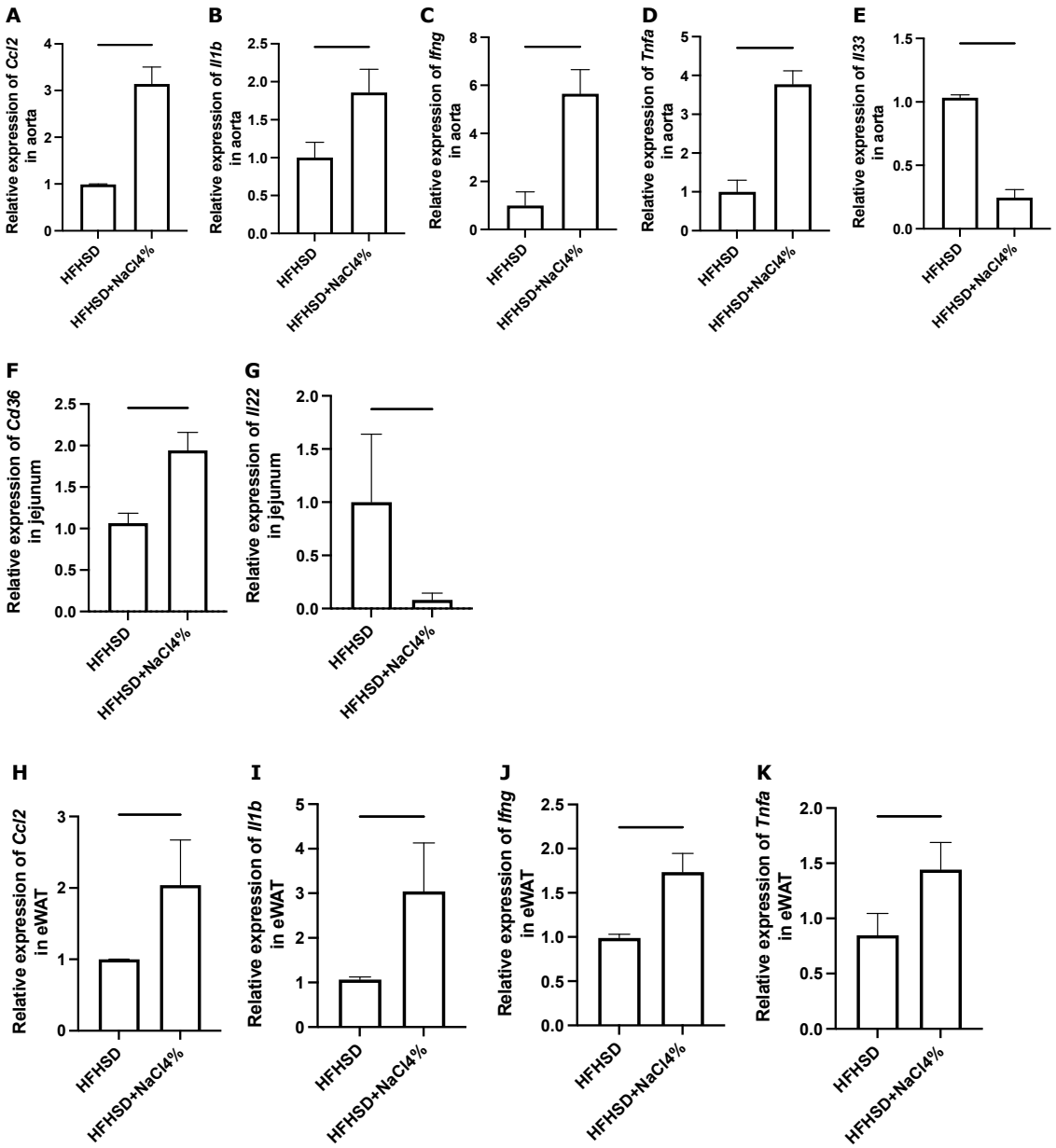

Fig. 3. Expression levels of genes related to inflammatory cytokines in the aorta and jejunum. Relative mRNA expression of (A) *Ccl2*, (B) *Il1b*, (C) *Ifng*, (D) *Tnfa*, and (E) *Il33* in the aorta, (F) *Cd36* and (G) *Il22* in the jejunum, and (H) *Ccl2*, (I) *Il1b*, (J) *Ifng*, and (K) *Tnfa* normalized to the expression of *Gapdh* ($n = 6$). Data are presented as mean ± SD values and analyzed using Welch's *t* tests; *$p<0.05$, **$p<0.01$, ***$p<0.001$, and ****$p<0.0001$. eWAT, epididymal white adipose tissue; HFHSD, high-fat high-sucrose diet; HFHSD + 4% NaCl, HFHSD and 4% gm NaCl.

Effects of HFHSD with high-salt loading on the expression of genes related to inflammatory cytokines in the aorta and with anti-inflammatory cytokines and fatty acid transporters in the jejunum. Gene expression of inflammatory cytokines and fatty acid transporters was analyzed using q-RT-PCR to determine the effect of HFHSD with high-salt loading on chronic inflammation. The expression levels of genes related to inflammatory cytokines, such as *Ccl2*, *Il1b*, *Ifng*, and *Tnfa*, in the aorta of the HFHSD + 4% NaCl group, were higher than those in the HFHSD group (Fig. 3A–D). In addition, the expression level of *Il33*, which is one of the factors that activate ILC2, in the aorta of the HFHSD + 4% NaCl group was lower than that of the HFHSD group (Fig. 3E). The *Cd36* expression level in the jejunum of the HFHSD + 4% NaCl group was higher than that of the HFHSD group (Fig. 3F), whereas the *Il22* expression level in the HFHSD + 4% NaCl group was lower than that in the HFHSD group (Fig. 3G). In the WAT, similar to the aorta, the expression levels of genes related to inflammatory cytokines in the HFHSD + 4% NaCl group were higher than those in the HFHSD group (Fig. 3H–K).

Effects of HFHSD with high-salt loading on the gut microbiota. We performed 16s rRNA sequencing to determine the effect of high-salt load HFHSD on the gut microbiota. The most abundant phylum was Bacteroidetes in both groups (HFHSD: 47.6 ± 8.1%, HFHSD + 4% NaCl: 52.1 ± 7.4%). The second and third most abundant phyla in the HFHSD group were Firmicutes and Proteobacteria, respectively, whereas those in the HFHSD + 4% NaCl group were Proteobacteria and Firmicutes, respectively (Fig. 4A and Table 2). Next, the F/B ratio, whose increase or decrease has been reported to be associated with various diseases, was calculated.[38–40] The F/B ratio in the HFHSD + 4% NaCl group was lower than that in the HFHSD group (Fig. 4B).

The Shannon index, Chao1 index, and Gini-Simpson index were used to assess the diversity of the gut microbiota, which revealed that the HFHSD + 4% NaCl group had lower diversity than the HFHSD group (Fig. 4C–E). PCoA plots of unweighted and weighted UniFrac distances were constructed to compare the two groups (Fig. 4F and G). The clustering results showed that the HFHSD and HFHSD + 4% NaCl groups belonged to different clusters.

Additionally, we used the LEfSe algorithm to identify specific taxa that were variably distributed between the two groups. Four taxa (including the class Bacteroidia, order *Bacteroidales*, and genus *Barnesiella*) were over-represented, and five taxa (including the class Alphaproteobacteria, genus *Streptococcus*, family *Lachnospiraceae*, family *Ruminococcaceae*, and genus *Allobaculum*) were under-represented in the HFHSD + 4% NaCl group compared to the HFHSD group (Fig. 4H).

Discussion

In this study using ApoE KO mice, we evaluated the effects of excessive salt intake on atherosclerosis development and showed that excessive salt intake alters the gut microbiota, increases the gene expression levels of long-chain fatty acid transporters in the small intestine, and the absorption of saturated fatty acids, thereby increasing serum saturated fatty acid levels, expanding atherosclerotic foci, and reducing anti-inflammatory innate cells.

Previous studies have reported that excessive intake of saturated fatty acids is associated with the development of atherosclerosis,[16] and that saturated fatty acids are rapidly taken up by cultured macrophages, potentially leading to a greater accumulation of arterial lipids.[41] In clinical practice, the current cardiovascular guidelines recommend reducing saturated fatty acids and replacing them with unsaturated fatty acids.[42] However, recent epidemiological studies have failed to reveal an increased risk of CVDs associated with diets high in saturated fat.[22] Furthermore, several studies have found no association between saturated fat intake and carotid intima-media thickness.[43] In contrast, high serum saturated fatty acid levels have been shown to increase the risk of coronary artery disease.[44] Taken together, these studies suggest that increased serum saturated fatty acid levels might be more strongly associated with atherosclerosis than saturated fatty acid intake. In the present study, although there was no difference in caloric intake between the HFHSD and HFHSD + 4% NaCl groups after pair feeding, serum lipid levels were significantly higher in the HFHSD + 4% NaCl group than in the HFHSD group. Based on these results, we evaluated the expression levels of genes related to inflammation in the small intestine to determine whether inflammation caused by a high-salt diet alters the dynamics of nutrient absorption from the intestinal tract. *Il22* mRNA levels in the small intestine of the HFHSD + 4% NaCl group were lower than those in the HFHSD group. IL22 is an important cytokine that plays a role in the thickening of the mucin layer of the small intestine and protects against intestinal inflammation by enhancing the expression of antimicrobial proteins in epithelial cells.[45] In contrast, *Cd36* mRNA levels, which are long-chain fatty acid transporters, increased following the administration of excessive salt in this study. In our previous study, we reported that dysbiosis caused by excessive intake of saturated fatty acids, sucrose, or trans-fatty acids causes inflammation in the intestinal tract, which in turn increases *Cd36* expression levels in the small intestine.[20] Dysbiosis is difficult to define precisely, but this study used changes in the F/B ratio and reduced diversity as markers. Increased F/B ratio has been reported to be associated with obesity,[39] whereas decreased the ratio has been reported to be associated with type 2 diabetes[40] and inflammatory bowel disease.[38] Moreover, Morgan, *et al.*[38] reported that the phylum Proteobacteria increased in IBD patients compared to healthy subjects. In this study, F/B ratio in the HFHSD + 4% NaCl group was lower than that in HFHSD group and the abundance of phylum Proteobacteria in the HFHSD + 4% NaCl group was higher than that in the HFHSD group. In summary, the excessive salt intake group in this study showed the gut microbiota more similar to IBD than to the gut microbiota that cause obesity and glucose intolerance.

Recently, other groups have reported that Cd36 expression in the small intestine is increased by dysbiosis and intestinal inflammation.[46] Shi *et al.*[47] have reported that the supplementation of *Bacteroides fragilis*, which is reported to be related with obesity, did not only deteriorated metabolic dysfunction but also increased the expression of Cd36 in small intestine. MUFAs, such as palmitoleic acid and oleic acid, in the aorta and sera of the HFHSD + 4% NaCl group were higher than those of the HFHSD group. MUFAs are found primarily in vegetable oils and have an unsaturated group with a single double bond in their structure. Randomized controlled trials have shown that MUFAs favorably regulate insulin sensitivity, blood pressure, and blood lipids, and prevent or improve the risk of metabolic syndrome and CVD.[48] MUFAs, like other long-chain fatty acids, are absorbed from Cd36 in the small intestine, therefore, the HFHSD + 4% NaCl group increased in the body, suggesting that their elimination in the stool may have decreased. In addition, it was suggested that there may be no correlation between serum concentrations of MUFA and atherosclerosis. Furthermore, in this study, the concentrations of PUFAs in feces, aorta, and sera were investigated and *n*-3 PUFAs, such as ALA, EPA and DHA, in the HFHSD + 4% NaCl group were lower than those in the HFHSD group. *n*-3 PUFAs have been reported to have anti-atherosclerotic effects, and the same was observed in this study.[49] DHA reduced tumor necrosis factor-α-induced monocyte adhesion to endothelial cells *in vitro* by decreasing expression of vascular cell adhesion molecule-1 and activation of nuclear factor kappa B, a key transcription factor involved in the regulation of inflammatory responses.[50] Furthermore, EPA and DHA act on macrophages and smooth muscle cells,[51–53] and have anti-atherosclerotic effects through stimulation of protective M2 macrophage polarity,[54] inhibition of modified LDL uptake by macrophages,[55] and inhibition of smooth muscle cell migration.[56]

The present study also suggested that inflammation in the intestine caused by a high-salt diet may have increased the gene expression of long-chain fatty acid transporters in the intestinal tract, resulting in increased saturated fatty acid absorption. Saturated fatty acid concentrations in visceral adipose tissue were also increased, with associated worsening of inflammation and lipolysis, resulting in a decrease in visceral adipose tissue and weight loss.[57,58]

As microorganisms rely on dietary substrates in the gut, the gut microbiota is often proposed as a mediator of the pro-and anti-inflammatory effects of diet. Similar to other nutrients, animal studies have demonstrated that salt-rich foods induce inflammation and autoimmunity through microbial mechanisms, such as the induction of T-helper 17 cells.[59] Moreover, type 3 innate lymphoid cells have been reported to have a function homologous to that of Th17, are very abundant in the intestinal mucosa, and play a role in intestinal homeostasis by producing interleukin (IL)-22 and IL-17 in response to IL-23 and IL-1β.[60]

In the 16s rRNA analyses of gut microbiota, the phylum Bacteroidetes, class Bacteroidia, order *Bacteroidales*, and genus *Barnesiella* were more abundant in HFHSD + 4% NaCl mice than in HFHSD mice. *Barnesiella*, a genus of the family Porphyromonadaceae and order *Bacteroidales*, is one of the most abundant genera detected in the mouse intestine. Several studies have revealed that the abundance of the phylum Bacteroidetes, class Bacteroidia, order *Bacteroidales*, family *Porphyromonadaceae*, and genus *Barnesiella* in diabetic (*db/db*) mice was higher than that in lean mice.[61,62] A previous study

doi: 10.3164/jcbn.24-163

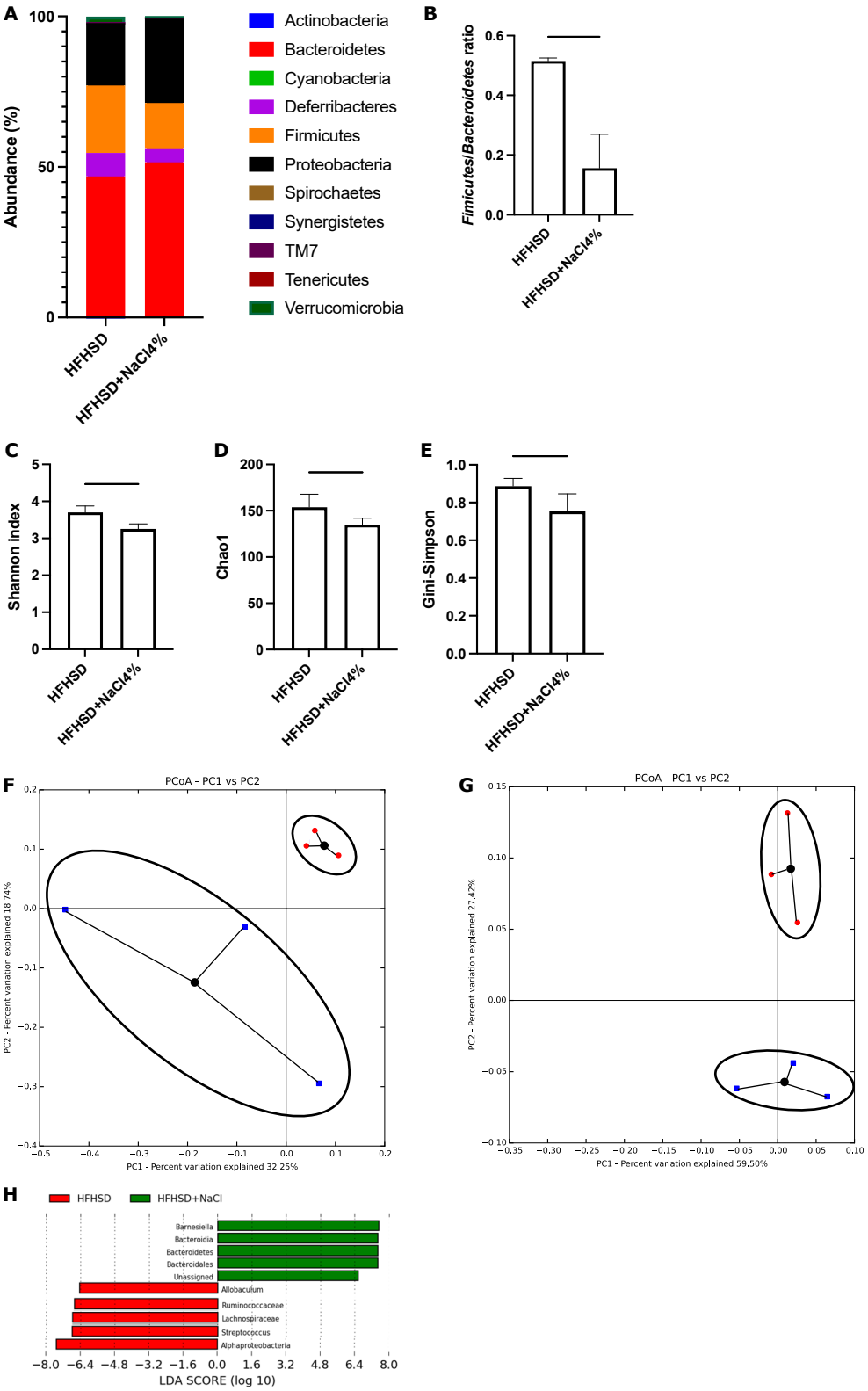

Fig. 4. 16s rRNA sequencing of the gut microbiota of the two groups of mice. (A) The relative abundance of phyla (%) ($n = 3$). Others included the phylum, such as Actinobacteria, Cyanobacteria, Spirochaetes, Synergistetes, TM7, and Tenericutes. (B) Firmicutes/Bacteroidetes ratio ($n = 3$). (C) Shannon index ($n = 3$). (D) Chao1 index ($n = 3$). (E) Gini-Simpson index ($n = 3$). (F) Unweighted PCoA plots ($n = 3$). (G) Weighted PCoA plots ($n = 3$). *K*-means clustering for gut microbiota is shown. *Red*, HFHSD group; *Blue*, HFHSD + 4% NaCl group. (H) Linear discriminant analysis (LDA) score (Log10) and LEfSe cladogram of HFHSD and HFHSD + 4% NaCl group ($n = 3$). (Red) taxa enriched in HFHSD group; (Green) taxa enriched in HFHSD + 4% NaCl group. Only taxa with a significant LDA threshold value >2 are shown. Data are presented as mean ± SD values and analyzed using Welch's *t* tests, *$p<0.05$, **$p<0.01$, and ***$p<0.001$. HFHSD, high-fat high-sucrose diet; HFHSD + 4% NaCl, HFHSD and 4% gm NaCl; LDA, linear discriminant analysis; LEfSe, LDA coupled with effect size; PCoA, principal coordinates analysis. See color figure in the on-line version.

Table 2. Relative abundance of phylum

	HFHSD	HFHSD + 4% NaCl	*p* value
Actinobacteria	0.23 (0.11)	0.00 (0.00)	0.009
Bacteroidetes	47.6 (8.1)	52.1 (7.4)	0.039
Cyanobacteria	0.02 (0.00)	0.00 (0.00)	0.321
Deferribacteres	7.78 (1.03)	4.64 (1.34)	0.044
Firmicutes	22.39 (8.06)	15.01 (1.81)	0.047
Proteobacteria	20.75 (3.32)	28.07 (2.50)	0.022
Spirochaetes	0.00 (0.00)	0.00 (0.00)	0.589
Synergistetes	0.00 (0.00)	0.00 (0.00)	0.407
TM7	0.14 (0.00)	0.02 (0.00)	0.406
Tenericutes	0.00 (0.00)	0.00 (0.00)	0.654
Verrucomicrobia	2.06 (0.23)	0.67 (0.00)	0.477

Data are expressed as mean (SD). Student's paired *t* test were conducted between two groups.

comparing the microbiota of patients with hypertension to healthy individuals has revealed that the abundance of the genus *Barnesiella* was higher in patients with hypertension.[7] In addition, the abundance of the genus *Barnesiella* increased in IL-22 deficient mice.[63] The function of the genus *Barnesiella* remains unclear; however, several previous studies and the present study suggest that the high-salt diet-induced increase in the genus *Barnesiella* is associated with dysbiosis, which might be related to a decrease in IL-22 in the intestinal tract.

Although the present study showed that a high-salt diet can promote the development of atherosclerosis, no obvious increase in blood pressure was detected. One possible reason for this observation is that in other studies of high-salt diet-induced atherosclerosis in ApoE KO mice, the dietary salt concentration was 7–8% gm and the administration period was 12 weeks.[64] In contrast, in our previous study, a high-salt diet of 8% gm resulted in extremely low food intake and frequent sudden death of mice during the 12-week treatment period; therefore, we reduced the salt concentration to 4% gm and shortened the treatment period to 8 weeks. Additionally, hypertension has long been known to increase the prevalence of coronary artery disease and the extent and severity of atherosclerosis in both humans[65,66] and animals.[67–69] In other words, we examined the effects of increased saturated fatty acid absorption on increased arterial stiffness while excluding the blood pressure component.

In this study, we investigated innate immune cells in the aorta. Previous studies have reported that ILC2 protects against atherosclerosis.[17,70] In addition, ILC2 transfer to ApoE KO mice reduced the lipid content of the atherosclerotic lesions.[17] In the present study, the number of ILC2 cells and the expression level of *Il33* in the aorta of the HFHSD + 4% NaCl group were lower than those of the HFHSD group. IL-33, which is secreted by ILC2 cells,[71] has been reported to play a protective role against the development of atherosclerosis.[72] The decrease in arterial ILC2 associated with excessive salt intake may exacerbate atherosclerosis by reducing the secretion of IL-33, which has anti-arterial effects.

As a limitation of this study, we did not reveal significant difference of blood pressure by excessive salt intake. However, a previous study showed that blood pressure did not change with high salt diet in the inactive phase but did in the active phase.[73] Therefore, re-measuring blood pressure during the active phase could show an increase in blood pressure due to the high-salt diet. In addition, in this study, the body weight of the HFHSD + 4% NaCl group was significantly lower than that of the HFHSD group. Furthermore, absolute and relative epididymal fat weights were lower than those of the HFHSD group. Previous studies have shown an inverse correlation between salt intake and body weight gain in mice fed a high-fat diet; DeClercq *et al.*[74] reported that excess salt intake increased epididymal fat weight in male mice, and Pitynski-Miller *et al.*[75] reported that excess salt intake in female rats. In summary, the effects of high-salt diets on body weight and visceral fat mass may vary among various backgrounds and require further study. On the other hand, in this study, excessive salt intake induced the inflammation in eWAT. In a previous study, expression of the inflammatory adipocytokines have been reported to increase in a dose-dependent manner upon salt treatment.[76] Furthermore, the inflammation in adipose tissue induces adipose tissue dysfunction such as decrease in fatty acid intake.[77] It has been reported that decreased fatty acid uptake into visceral fat increases ectopic fat accumulation, whereas visceral adipose tissue weight decreases. Since atherosclerosis, a form of ectopic fat accumulation, was advanced in this study, the decrease in body weight in the HFHSD + 4% NaCl group may have been due in part to a reduction in visceral fat weight caused by inflammation within visceral fat. Furthermore, we have not evaluated factors involved in atherosclerosis, such as glucose tolerance,[78] trimethylamine oxide in serum,[79] short-chain fatty acids,[80] and lipopolysaccharides.[81] Additional data on them might have further elaborated on how excessive salt intake causes abnormalities in intestinal bacteria and contributes to the progression of atherosclerosis. Only male mice were employed in this study. This was because, while this study focused on the modification of innate immunity, our previous study reported that sex hormones modify innate immunity.[28] Therefore, we employed male mice, which have fewer differences in sex hormones due to the sex cycle. However, future studies in female mice are needed, as sex differences in fatty acid metabolism and salt sensitivity of the gut microbiota have been reported.[82] Lastly, we did not have the data of the characterization of the initial fecal sample prior feeding. If we had the data, we could compare the data with the baseline data and more accurately determine the changes in the gut microbiota due to differences in the diet.

In conclusion, this study revealed the mechanism by which an HFHSD that mimics the modern diet, loaded with excess salt promotes the development of atherosclerosis. We revealed that excessive salt intake causes alterations in the gut microbiota, induces inflammation in the gut, increases the expression of long-chain fatty acid transporters in the small intestine, and increases the influx of saturated fatty acids into the body, thereby worsening atherosclerosis. This study offers insights into the mechanism of aggravation of atherosclerosis which could not be explained by an increase in saturated fatty acid intake alone.

Acknowledgments

We would like to thank Editage (www.editage.com) for English language editing. Emi Ushigome received grant support from the Japan Society for the Promotion of Science (grant numbers 18K15897 and 22K08108).

Conflict of Interest

EU received grant support from the Japanese Study Group for Physiology and Management of Blood Pressure, the Astellas Foundation for Research on Metabolic Disorders (Grant number: 4024), Mishima Kaiun Memorial Foundation, and received personal fees from Nippon Boehringer Ingelheim Co., Ltd., Mitsubishi Tanabe Pharma Corporation, Daiichi Sankyo Co., Ltd, MSD K.K., Kyowa Hakko Kirin Co., Ltd., Sumitomo Dainippon Pharma Co., Ltd., Kowa Pharmaceutical Co., Ltd., Novo Nordisk Pharma Ltd., Ono Pharmaceutical Co., Ltd., Taisho Pharmaceutical Co., Ltd., and Sanofi K.K., outside the submitted work. Donated Fund Laboratory of Diabetes therapeutics is an endowment department, supported with an unrestricted grant from Ono

doi: 10.3164/jcbn.24-163

Pharmaceutical Co., Ltd., Taiyo Kagaku Co. Ltd., and Taisho Pharmaceutical Co., Ltd. NN received personal fees from Kowa Pharmaceutical Co. Ltd., and Novo Nordisk Pharma Ltd., Nippon Boehringer Ingelheim Co. Ltd., Terumo Corp. MH received grants from AstraZeneca K.K., Ono Pharma Co. Ltd., Kowa Pharma Co. Ltd., and received personal fees from AstraZeneca K.K., Ono Pharma Co. Ltd., Eli Lilly, Japan, Sumitomo Dainippon Pharma Co., Ltd., Daiichi Sankyo Co. Ltd., Mitsubishi Tanabe Pharma Corp., Sanofi K.K., and Kowa Pharma Co. Ltd. outside of the submitted work. MF received grants from Ono Pharma Co. Ltd., Oishi Kenko inc., Yamada Bee Farm, Nippon Boehringer Ingelheim Co. Ltd., Kissei Pharma Co. Ltd., Mitsubishi Tanabe Pharma Corp., Daiichi Sankyo Co. Ltd., Sanofi K.K., Takeda Pharma Co. Ltd., Astellas Pharma Inc., MSD K.K., Kyowa Kirin Co., Ltd., Sumitomo Dainippon Pharma Co., Ltd., Kowa Pharma Co. Ltd., Novo Nordisk Pharma Ltd., Sanwa Kagagu Kenkyusho CO., Ltd., Eli Lilly, Japan, K.K., Taisho Pharma Co., Ltd., Terumo Corp., Tejin Pharma Ltd., Nippon Chemiphar Co., Ltd., Abbott Japan Co. Ltd., and Johnson & Johnson K.K. Medical Co., Terumo Corp., and received personal fees from Nippon Boehringer Ingelheim Co., Ltd., Kissei Pharma Co., Ltd., Mitsubishi Tanabe Pharma Corp., Daiichi Sankyo Co. Ltd., Sanofi K.K., Takeda Pharma Co. Ltd., Astellas Pharma Inc., MSD K.K., Kyowa Kirin Co. Ltd., Sumitomo Dainippon Pharma Co. Ltd., Kowa Pharma Co. Ltd., Novo Nordisk Pharma Ltd., Ono Pharma Co. Ltd., Sanwa Kagaku Kenkyusho Co. Ltd., Eli Lilly Japan K.K., Taisho Pharma Co., Ltd., Bayer Yakuhin, Ltd., AstraZeneca K.K., Mochida Pharma Co. Ltd., Abbott Japan Co. Ltd., Teijin Pharma Ltd., Arkray Inc., Medtronic Japan Co. Ltd., Nipro Corp., and Terumo Corp., outside the submitted work.

References

1 Duttaroy AK. Role of gut microbiota and their metabolites on atherosclerosis, hypertension and human blood platelet function: a review. *Nutrients* 2021; **13**: 144.
2 Marchio P, Guerra-Ojeda S, Vila JM, Aldasoro M, Victor VM, Mauricio MD. Targeting early atherosclerosis: a focus on oxidative stress and inflammation. *Oxid Med Cell Longev* 2019; **2019**: 8563845.
3 Cumpston M, Li T, Page MJ, *et al*. Updated guidance for trusted systematic reviews: a new edition of the Cochrane Handbook for Systematic Reviews of Interventions. *Cochrane Database Syst Rev* 2019; **10**: ED000142.
4 Ma Z, Hummel SL, Sun N, Chen Y. From salt to hypertension, what is missed? *J Clin Hypertens (Greenwich)* 2021; **23**: 2033–2041.
5 Itoh N, Tsuya A, Togashi H, *et al*. Increased salt intake is associated with diabetes and characteristic dietary habits: a community-based cross-sectional study in Japan. *J Clin Biochem Nutr* 2022; **71**: 143–150.
6 Seck EH, Senghor B, Merhej V, *et al*. Salt in stools is associated with obesity, gut halophilic microbiota and *Akkermansia muciniphila* depletion in humans. *Int J Obes (Lond)* 2019; **43**: 862–871.
7 Dan X, Mushi Z, Baili W, *et al*. Differential analysis of hypertension-associated intestinal microbiota. *Int J Med Sci* 2019; **16**: 872–881.
8 Miranda PM, De Palma G, Serkis V, *et al*. High salt diet exacerbates colitis in mice by decreasing Lactobacillus levels and butyrate production. *Microbiome* 2018; **6**: 57.
9 Ross R. Atherosclerosis—an inflammatory disease. *N Engl J Med* 1999; **340**: 115–126.
10 Bernstein CN, Wajda A, Blanchard JF. The incidence of arterial thromboembolic diseases in inflammatory bowel disease: a population-based study. *Clin Gastroenterol Hepatol* 2008; **6**: 41–45.
11 Kristensen SL, Ahlehoff O, Lindhardsen J, *et al*. Disease activity in inflammatory bowel disease is associated with increased risk of myocardial infarction, stroke and cardiovascular death—a Danish nationwide cohort study. *PLoS One* 2013; **8**: e56944.
12 Kirchgesner J, Beaugerie L, Carrat F, *et al*. Increased risk of acute arterial events in young patients and severely active IBD: a nationwide French cohort study. *Gut* 2018; **67**: 1261–1268.
13 González-Becerra K, Ramos-Lopez O, Barrón-Cabrera E, *et al*. Fatty acids, epigenetic mechanisms and chronic diseases: a systematic review. *Lipids Health Dis* 2019; **18**: 178.
14 Te Morenga L, Montez JM. Health effects of saturated and trans-fatty acid intake in children and adolescents: systematic review and meta-analysis. *PLoS One* 2017; **12**: e0186672.
15 Gaudreault N, Kumar N, Posada JM, *et al*. ApoE suppresses atherosclerosis by reducing lipid accumulation in circulating monocytes and the expression of inflammatory molecules on monocytes and vascular endothelium. *Arterioscler Thromb Vasc Biol* 2012; **32**: 264–272.
16 Degirolamo C, Shelness GS, Rudel LL. LDL cholesteryl oleate as a predictor for atherosclerosis: evidence from human and animal studies on dietary fat. *J Lipid Res* 2009; **50 Suppl**: S434–S439.
17 Mantani PT, Dunér P, Ljungcrantz I, Nilsson J, Björkbacka H, Fredrikson GN. ILC2 transfers to apolipoprotein E deficient mice reduce the lipid content of atherosclerotic lesions. *BMC Immunol* 2019; **20**: 47.
18 Okamura T, Hamaguchi M, Mori J, *et al*. Partially hydrolyzed guar gum suppresses the development of sarcopenic obesity. *Nutrients* 2022; **14**: 1157.
19 Piedrahita JA, Zhang SH, Hagaman JR, Oliver PM, Maeda N. Generation of mice carrying a mutant apolipoprotein E gene inactivated by gene targeting in embryonic stem cells. *Proc Natl Acad Sci U S A* 1992; **89**: 4471–4475.
20 Okamura T, Hashimoto Y, Majima S, *et al*. Trans fatty acid intake induces intestinal inflammation and impaired glucose tolerance. *Front Immunol* 2021; **12**: 669672.
21 Kawai S, Takagi Y, Kaneko S, Kurosawa T. Effect of three types of mixed anesthetic agents alternate to ketamine in mice. *Exp Anim* 2011; **60**: 481–487.
22 Dehghan M, Mente A, Zhang X, *et al*. Associations of fats and carbohydrate intake with cardiovascular disease and mortality in 18 countries from five continents (PURE): a prospective cohort study. *Lancet* 2017; **390**: 2050–2062.
23 Yuan Z, Kishimoto C, Sano H, Shioji K, Xu Y, Yokode M. Immunoglobulin treatment suppresses atherosclerosis in apolipoprotein E-deficient mice via the Fc portion. *Am J Physiol Heart Circ Physiol* 2003; **285**: H899–H906.
24 Hu D, Yin C, Mohanta SK, Weber C, Habenicht AJ. Preparation of single cell suspensions from mouse aorta. *Bio Protoc* 2016; **6**: e1832.
25 Molofsky AB, Nussbaum JC, Liang H-E, *et al*. Innate lymphoid type 2 cells sustain visceral adipose tissue eosinophils and alternatively activated macrophages. *J Exp Med* 2013; **210**: 535–549.
26 Wang S, Li J, Wu S, *et al*. Type 3 innate lymphoid cell: a new player in liver fibrosis progression. *Clin Sci* 2018; **132**: 2565–2582.
27 Ono Y, Nagai M, Yoshino O, *et al*. CD11c+ M1-like macrophages (MΦs) but not CD206+ M2-like MΦ are involved in folliculogenesis in mice ovary. *Sci Rep* 2018; **8**: 8171.
28 Okamura T, Hamaguchi M, Bamba R, *et al*. Immune modulating effects of additional supplementation of estradiol combined with testosterone in murine testosterone-deficient NAFLD model. *Am J Physiol Gastrointest Liver Physiol* 2020; **318**: G989–G999.
29 Livak KJ, Schmittgen TD. Analysis of relative gene expression data using real-time quantitative PCR and the $2^{-\Delta\Delta C_T}$ Method. *Methods* 2001; **25**: 402–408.
30 Caporaso JG, Kuczynski J, Stombaugh J, *et al*. QIIME allows analysis of high-throughput community sequencing data. *Nat Methods* 2010; **7**: 335–336.
31 Edgar RC. Search and clustering orders of magnitude faster than BLAST. *Bioinformatics* 2010; **26**: 2460–2461.
32 Coburn CT, Knapp FF Jr, Febbraio M, Beets AL, Silverstein RL, Abumrad NA. Defective uptake and utilization of long chain fatty acids in muscle and adipose tissues of CD36 knockout mice. *J Biol Chem* 2000; **275**: 32523–32529.
33 Shannon CE. A mathematical theory of communication. *Bell Syst Tech J* 1948; **27**: 379–423.
34 Chao A, Chazdon RL, Colwell RK, Shen TJ. Abundance-based similarity indices and their estimation when there are unseen species in samples. *Biometrics* 2006; **62**: 361–371.
35 Simpson EH. Measurement of diversity. *Nature* 1949; **163**: 688.
36 Sanguinetti G, Milo M, Rattray M, Lawrence ND. Accounting for probe-level noise in principal component analysis of microarray data. *Bioinformatics*

2005; **21**: 3748–3754.
37 Segata N, Izard J, Waldron L, *et al*. Metagenomic biomarker discovery and explanation. *Genome Biol* 2011; **12**: R60.
38 Morgan XC, Tickle TL, Sokol H, *et al*. Dysfunction of the intestinal microbiome in inflammatory bowel disease and treatment. *Genome Biol* 2012; **13**: R79.
39 Ley RE, Turnbaugh PJ, Klein S, Gordon JI. Microbial ecology: human gut microbes associated with obesity. *Nature* 2006; **444**: 1022–1023.
40 Larsen N, Vogensen FK, van den Berg FW, *et al*. Gut microbiota in human adults with type 2 diabetes differs from non-diabetic adults. *PLoS One* 2010; **5**: e9085.
41 De Pascale C, Avella M, Perona JS, Ruiz-Gutierrez V, Wheeler-Jones CP, Botham KM. Fatty acid composition of chylomicron remnant-like particles influences their uptake and induction of lipid accumulation in macrophages. *FEBS J* 2006; **273**: 5632–5640.
42 Sacks FM, Lichtenstein AH, Wu JHY, *et al*. Dietary fats and cardiovascular disease: a presidential advisory from the American Heart Association. *Circulation* 2017; **136**: e1–e23.
43 Virtanen JK, Mursu J, Virtanen HEK, *et al*. Associations of egg and cholesterol intakes with carotid intima-media thickness and risk of incident coronary artery disease according to apolipoprotein E phenotype in men: the Kuopio Ischaemic Heart Disease Risk Factor Study. *Am J Clin Nutr* 2016; **103**: 895–901.
44 Chei CL, Yamagishi K, Kitamura A, *et al*. Serum fatty acid and risk of coronary artery disease—Circulatory Risk in Communities Study (CIRCS). *Circ J* 2018; **82**: 3013–3020.
45 Sonnenberg GF, Fouser LA, Artis D. Border patrol: regulation of immunity, inflammation and tissue homeostasis at barrier surfaces by IL-22. *Nat Immunol* 2011; **12**: 383–390.
46 Indiani CMDSP, Rizzardi KF, Castelo PM, Ferraz LFC, Darrieux M, Parisotto TM. Childhood obesity and Firmicutes/Bacteroidetes ratio in the gut microbiota: a systematic review. *Child Obes* 2018; **14**: 501–509.
47 Shi G, Lin Y, Wu Y, *et al*. *Bacteroides fragilis* supplementation deteriorated metabolic dysfunction, inflammation, and aorta atherosclerosis by inducing gut microbiota dysbiosis in animal model. *Nutrients* 2022; **14**: 2199.
48 Gillingham LG, Harris-Janz S, Jones PJH. Dietary monounsaturated fatty acids are protective against metabolic syndrome and cardiovascular disease risk factors. *Lipids* 2011; **46**: 209–228.
49 Takashima A, Fukuda D, Tanaka K, *et al*. Combination of n-3 polyunsaturated fatty acids reduces atherogenesis in apolipoprotein E-deficient mice by inhibiting macrophage activation. *Atherosclerosis* 2016; **254**: 142–150.
50 Wang TM, Chen CJ, Lee TS, *et al*. Docosahexaenoic acid attenuates VCAM-1 expression and NF-κB activation in TNF-α-treated human aortic endothelial cells. *J Nutr Biochem* 2011; **22**: 187–194.
51 Moss JWE, Williams JO, Ramji DP. Nutraceuticals as therapeutic agents for atherosclerosis. *Biochim Biophys Acta Mol Basis Dis* 2018; **1864 (5 Pt A)**: 1562–1572.
52 Moss JWE, Ramji DP. Nutraceutical therapies for atherosclerosis. *Nat Rev Cardiol* 2016; **13**: 513–532.
53 Moss JWE, Davies TS, Garaiova I, Plummer SF, Michael DR, Ramji DP. A unique combination of nutritionally active ingredients can prevent several key processes associated with atherosclerosis *in vitro*. *PLoS One* 2016; **11**: e0151057.
54 Chang HY, Lee HN, Kim W, Surh YJ. Docosahexaenoic acid induces M2 macrophage polarization through peroxisome proliferator-activated receptor γ activation. *Life Sci* 2015; **120**: 39–47.
55 McLaren JE, Michael DR, Guschina IA, Harwood JL, Ramji DP. Eicosapentaenoic acid and docosahexaenoic acid regulate modified LDL uptake and macropinocytosis in human macrophages. *Lipids* 2011; **46**: 1053–1061.
56 Mizutani M, Asano M, Roy S, *et al*. ω-3 polyunsaturated fatty acids inhibit migration of human vascular smooth muscle cells *in vitro*. *Life Sci* 1997; **61**: PL269–PL274.
57 Okamura T, Hashimoto Y, Mori J, *et al*. ILC2s improve glucose metabolism through the control of saturated fatty acid absorption within visceral fat. *Front Immunol* 2021; **12**: 669629.
58 Schwartz EA, Reaven PD. Lipolysis of triglyceride-rich lipoproteins, vascular inflammation, and atherosclerosis. *Biochim Biophys Acta* 2012; **1821**: 858–866.
59 Aguiar SLF, Miranda MCG, Guimarães MAF, *et al*. High-salt diet induces IL-17-dependent gut inflammation and exacerbates colitis in mice. *Front Immunol* 2018; **8**: 1919.
60 Forkel M, Mjösberg J. Dysregulation of group 3 innate lymphoid cells in the pathogenesis of inflammatory bowel disease. *Curr Allergy Asthma Rep* 2016; **16**: 73.
61 Cani PD, Neyrinck AM, Fava F, *et al*. Selective increases of bifidobacteria in gut microflora improve high-fat-diet-induced diabetes in mice through a mechanism associated with endotoxaemia. *Diabetologia* 2007; **50**: 2374–2383.
62 Cani PD, Amar J, Iglesias MA, *et al*. Metabolic endotoxemia initiates obesity and insulin resistance. *Diabetes* 2007; **56**: 1761–1772.
63 Zenewicz LA, Yin X, Wang G, *et al*. IL-22 deficiency alters colonic microbiota to be transmissible and colitogenic. *J Immunol* 2013; **190**: 5306–5312.
64 Ketonen J, Merasto S, Paakkari I, Mervaala EMA. High sodium intake increases vascular superoxide formation and promotes atherosclerosis in apolipoprotein E-deficient mice. *Blood Press* 2005; **14**: 373–382.
65 Solberg LA, Strong JP. Risk factors and atherosclerotic lesions. A review of autopsy studies. *Arteriosclerosis* 1983; **3**: 187–198.
66 Restrepo C, Montenegro MR, Solberg LA. Atherosclerosis in persons with selected diseases. *Lab Invest* 1968; **18**: 552–559.
67 Moses C. Development of atherosclerosis in dogs with hypercholesterolemia and chronic hypertension. *Circ Res* 1954; **2**: 243–247.
68 McGill HC Jr, Carey KD, McMahan CA, *et al*. Effects of two forms of hypertension on atherosclerosis in the hyperlipidemic baboon. *Arteriosclerosis* 1985; **5**: 481–493.
69 Chobanian AV., Lichtenstein AH, Nilakhe V, Haudenschild CC, Drago R, Nickerson C. Influence of hypertension on aortic atherosclerosis in the Watanabe rabbit. *Hypertension* 1989; **14**: 203–209.
70 Newland SA, Mohanta S, Clément M, *et al*. Type-2 innate lymphoid cells control the development of atherosclerosis in mice. *Nat Commun* 2017; **8**: 15781.
71 Huang Y, Guo L, Qiu J, *et al*. IL-25-responsive, lineage-negative KLRG1^{hi} cells are multipotential 'inflammatory' type 2 innate lymphoid cells. *Nat Immunol* 2015; **16**: 161–169.
72 Miller AM, Xu D, Asquith DL, *et al*. IL-33 reduces the development of atherosclerosis. *J Exp Med* 2008; **205**: 339–346.
73 Combe R, Mudgett J, El Fertak L, *et al*. How does circadian rhythm impact salt sensitivity of blood pressure in mice? A study in two close C57Bl/6 substrains. *PLoS One* 2016; **11**: e0153472.
74 DeClercq VC, Goldsby JS, McMurray DN, Chapkin RS. Distinct adipose depots from mice differentially respond to a high-fat, high-salt diet. *J Nutr* 2016; **146**: 1189–1196.
75 Pitynski-Miller D, Ross M, Schmill M, *et al*. A high salt diet inhibits obesity and delays puberty in the female rat. *Int J Obes (Lond)* 2017; **41**: 1685–1692.
76 Lee M, Sorn SR, Lee Y, Kang I. Salt induces adipogenesis/lipogenesis and inflammatory adipocytokines secretion in adipocytes. *Int J Mol Sci* 2019; **20**: 160.
77 Longo M, Zatterale F, Naderi J, *et al*. Adipose tissue dysfunction as determinant of obesity-associated metabolic complications. *Int J Mol Sci* 2019; **20**: 2358.
78 Temelkova-Kurktschiev TS, Koehler C, Henkel E, Leonhardt W, Fuecker K, Hanefeld M. Postchallenge plasma glucose and glycemic spikes are more strongly associated with atherosclerosis than fasting glucose or HbA1c level. *Diabetes Care* 2000; **23**: 1830–1834.
79 Wang Z, Klipfell E, Bennett BJ, *et al*. Gut flora metabolism of phosphatidylcholine promotes cardiovascular disease. *Nature* 2011; **472**: 57–63.
80 Mathew OP, Ranganna K, Milton SG. Involvement of the antioxidant effect and anti-inflammatory response in butyrate-inhibited vascular smooth muscle cell proliferation. *Pharmaceuticals (Basel)* 2014; **7**: 1008–1027.
81 Lehr HA, Sagban TA, Ihling C, *et al*. Immunopathogenesis of atherosclerosis: endotoxin accelerates atherosclerosis in rabbits on hypercholesterolemic diet. *Circulation* 2001; **104**: 914–920.
82 Razavi AC, Potts KS, Kelly TN, Bazzano LA. Sex, gut microbiome, and cardiovascular disease risk. *Biol Sex Differ* 2019; **10**: 29.

doi: 10.3164/jcbn.24-163